

## Investigating dynamic and static aspects of regional sea level changes in the north-western Indian Ocean

N. ESHGHI, A. BARZANDEH, F. HOSSEINIBALAM and S. HASSANZADEH

*Department of Physics, University of Isfahan, Iran*

(Received: 8 December 2018; accepted: 3 September 2019)

**ABSTRACT** Regional sea level changes were studied in the North-West Indian Ocean (NWIO). Basically, the processes affecting regional sea level changes can be divided into dynamic and quasi-static components. In the present study, dynamic sea level changes were evaluated by applying statistical methods such as Trend, Empirical Orthogonal Function (EOF), Spectral and Correlation analyses to the mean sea level anomaly, surface heat flux, and wind stress data. In addition, quasi-static sea level changes were examined by considering the inverted barometer effect. The results indicated that the maximum sea level rise is mostly observed in areas adjacent to the Gulf of Aden, and the minimum sea level rise is seen at the centre of the region, near the equator and oriented towards the SW. In general, in NWIO, the main factors affecting sea level changes are weakened and intensified with a one-year period. The correlation coefficients of heat flux and wind stress with the 2nd EOF of the sea level are larger than those of other modes so that the effect of internal factors, such as seasonal change, is, generally, smaller than the effect of external factors such as El-Nino - Southern Oscillation. The direction of prevailing winds in the region causes the positive sea level anomalies by Ekman suction and increasing the depth of the tropical thermocline. The inverted barometer effect on the sea level changes is significant in most of the months, except December, in such a way that it decreases in the cold months by moving towards high latitudes, while increases in warm months by moving to high latitudes. The distribution of non-barometric effects in the Arabian Sea indicates that they are caused by interactions with the Indian Ocean mostly from the southern areas of the Arabian Sea and the intensity of these effects decreases northwards and westwards during the year.

**Key words:** regional sea level change, statistical analysis, heat flux, wind stress, inverted barometer effect.

### 1. Introduction

Sea level is one of the most important oceanic parameters which can be a good indicator of climate change and describes oceanic states over different time periods, especially long-term trends. Global warming has increased the temperature of the oceans and melted ice sheets, both of which have resulted in global mean sea level rise. Various studies such as Gornitz (1995), Church *et al.* (2001) and Antonov *et al.* (2005) have illustrated that the sea level rise in the 20th century has been measured based on the analysis of tide gauge data. Changes in the atmospheric and

oceanic properties affect the sea level anomalies so that these effects are dependent on the spatial and temporal intervals. In addition, to examining the global mean sea level trends, assessments and surveys on sea level fluctuations are also taking place on a regional scale. For this purpose, some researches have been conducted on the sea level rise in the Indian Ocean because it is the hottest oceanic region in the world. In studies such as Douglas (1991), Shankar and Shetye (1999), and Unnikrishnan and Shankar (2007), using the mean sea level data from tide gauge, the long-term sea level trend is investigated and its incremental rate is estimated. Church *et al.* (2004) determined a rate of 2 mm/year in the sea level rise of the northern parts of the Indian Ocean, except for the northern parts of the Bay of Bengal whose rate was as 4 mm/year. Overall, in all previous studies, there is a consensus that there are large rates of sea level rise over the Indian Ocean, and recent developments in satellite oceanography can also provide a new vision for estimating changes in mean sea level in terms of climate changes. Sea level anomalies on a regional scale, on one hand, are affected by the global climate change and, on the other hand, by abnormal local climate changes (Church *et al.*, 2006). For example, Barzandeh *et al.* (2018) showed that the sea level anomaly responds to wind-driven coastal upwelling, as a regional phenomenon, in the Persian Gulf.

Basically, the processes affecting regional sea level changes can be divided into dynamic and quasi-static components (Stammer *et al.*, 2013). Dynamic regional sea level changes are highly variable in space and time, and can result in substantial variability in sea level on interannual to decadal timescales superimposed on longer-term trends. Dynamic regional sea level can reasonably be considered as barotropic and steric changes. Barotropic changes (the ocean's response to regional winds) are associated with regional changes in the ocean mass due to changes in oceanic barotropic flows, so that barotropic redistribution of mass is important for dynamic sea level changes on intra-annual time scales. On interannual time scales, barotropic changes play a role in the high latitudes and over shallow shelf seas, but in most other regions, dynamic sea level changes are largely steric in nature. Steric sea level changes occur under the influence of thermal expansion and salinity changes (Jordà and Gomis, 2013; Roberts *et al.*, 2016). From another point of view, there are two factors affecting the dynamic mean sea level changes on a regional scale: the surface heat flux and wind stress (Gill, 1982). The wind stress anomalies cause a change in the convergence of the near-surface Ekman transport (Timmermann *et al.*, 2010). Furthermore, variability of the upper ocean heat content in the tropics has strong effects on the regional sea level anomalies. The surface heat flux affects the thermodynamic conditions of sea surface waters and sea level changes. But the degree of sea level influence from the surface heat flux in different oceanic basins is different (Bouttes *et al.*, 2014; Gera *et al.*, 2016; Ruiz Etcheverry *et al.*, 2016). Historically, regional sea level changes were interpreted as being primarily thermosteric in nature, reflecting changes in the ocean's heat (Levitus *et al.*, 2000). Therefore, the study of the effect of heat flux on regional sea level changes can indirectly include the effect of thermosteric component. On the other hand, not all components of regional sea level changes are dynamic in nature. In particular, the response to several types of ocean loading can lead to quasi-static variability. One of the most important of these is the inverted barometer effects. The inverted barometer signal appears due to the response of the ocean to the atmospheric pressure in sea level anomalies. Analysis of the ocean stratification suggests that there is always a quasi-static inverted barometric signal in the boundary layer of the air-sea interactions in different frequencies and ranges of sea-level anomalies. The inverted barometer effects can overwhelm annual sea

level changes in a region. In certain tropical regions affected by the western boundary current, by using methods based on the processing and decomposing of sea level signals, the effect of the inverted barometer on sea level may not be as expected because of the multiplicity of factors affecting sea level and the probability of mixing co-frequent signals. In fact, due to large pressures generated by waves and currents relative to atmospheric pressures, the inverted barometer signal in all oceanic conditions is not recognisable and processable, while the inverted barometer effect on sea level changes is not long-term (Wunsch and Stammer, 1997; Mathers and Woodworth, 2004; Sturges and Douglas, 2011; Piecuch *et al.*, 2016b). So far, few studies have been conducted on the inverted barometer effect and its regional variations. Goring (1995) investigated the sea level response to atmospheric pressure for a period shorter than one month for New Zealand. According to his data and analysis, sea level generally responds to barometric pressure changes after a few hours (depending on the region, it may take 3-4 hours). Investigating the tidal gauge data, Ponte (2006) found that in spite of the inverted barometer signal, the extent of contributing of this effect in several regions is very different so that the standard deviation of the inverted barometer was obtained from 1 cm in the tropics to more than 7 cm in the polar regions. Statistical analysis illustrated that the inverted barometer signals were important in the sea level variance, especially at mid- and high-latitudes, and the changes in the inverted barometer effect in the Indian Ocean tropical regions are seasonal. Piecuch and Ponte (2015) probed the effect of the inverted barometer on recent changes in sea level on the coasts of North America. According to the study, about 25% of the interannual sea level changes are due to the inverted barometer effect.

### 1.1. Study area

This study focuses on the Arabian Sea (43-78° E; 8-26° N), a region characterised by strong seasonal and interannual changes in salinity and temperature and, with regard to its complex interactions of the masses, complex seasonal turns and adjacency to coasts, bays, and islands were considered. This region, covering all three basins of the Arabian Sea, the Gulf of Oman, and the Gulf of Aden, is called North-West Indian Ocean (NWIO) basin. Significant features of NWIO include the seasonal effects of SW and NE monsoons such as surface flows. Monsoonal climate dominates the northern Indian Ocean. Annual mean distributions of atmospheric and oceanic parameters are, therefore, of only limited use. In general, strong winds blow from SW to NE during the summer monsoon and they blow from NW to SE during the winter monsoons. It is characterised by high pressure over the Asian land mass and north-easterly winds over the tropics and northern subtropics while air pressure gradients over the ocean are small. Winds blow steadily over the entire western Indian Ocean north of the equator. The stronger winds of the Summer Monsoon season dominate the annual mean in the northern Indian Ocean as well. This produces a net south-westerly stress over the north-western Indian Ocean and in particular along the east African coast. Mean winds along the equator are weak and westerly (Shetye *et al.*, 1991, 1994; Gera *et al.*, 2016). Also, there is an irregular oscillation of sea-surface temperatures, called Indian Ocean Dipole (IOD), in which the western Indian Ocean becomes alternately warmer and then colder than the eastern part of the ocean (Saji *et al.* 1999). But all the systems affecting the NWIO's climatic and oceanographic conditions are not limited to the existing conditions and phenomena within the Indian Ocean basin and it is sometimes affected by global climatological phenomena or oceanic systems in the Pacific and the Atlantic regions. For example, the El Niño - Southern Oscillation (ENSO) will induce warming in the NWIO with a lag of one season (Du *et al.*, 2009).

The exchange of flows will be caused by changes in sea level. Consequently, studying the mean sea level for this area can be considered important. In addition, this area is surrounded by coasts from all geographical directions, except from the south. In fact, the small size of the study area relative to the Atlantic, Pacific, and Indian Ocean basins, has caused its coastal regime to be drawn along the two sides of the triangular Arabian Sea basin and covers approximately 25% of the total region. Thus, by examining the distribution of regional sea level changes, the ratio of the coastal regime and the exchange of free oceanic waters can be found in the tropical regions of southern Arabian Sea. In addition, the importance of the effects of other climatic phenomena such as the IOD on the physical conditions of the ocean can add to the need to study quantities such as sea level in the area. Circulation of the weak monsoons in NWIO and the decrease in the cloud cover will increase the surface heat flux in the northern Indian Ocean, causing heat expansion and rising sea levels (Qasim, 1982; Shukla, 1987a).

The aim of this study is:

1. to evaluate the prevailing sea level changes and its linear temporal trend in NWIO;
2. to study the factors affecting the dynamic regional sea level changes such as heat flux and wind stress in NWIO;
3. to examine the inverted barometer effect on the sea level anomalies as the quasi-static component of regional sea level changes in NWIO.

## 2. Materials and methods

First of all, the sea level anomaly data were extracted from the Aviso (MSLA-H Ssalto/Duacs altimeter products from <https://www.aviso.altimetry.fr/>) with a resolution of  $0.25 \times 0.25^\circ$  along the latitude and longitude, and in the monthly mean 1993-2015. Then, simple trend analysis was conducted on the extracted data set by estimating slopes of fitted lines on the time series of data for each spatial grid-point.

The Tropflux data were used for analysing heat flux in the study area. This data set, supplied by ESSO INCOIS (Indian National Centre for Ocean Information Services) includes gridded data of sea surface fluxes with  $1 \times 1^\circ$  resolution and in the monthly mean 1979-2016 (Kumar *et al.*, 2012).

The wind speed data were extracted from the ECMWF (European Centre for Medium-Range Weather Forecasts), with  $0.25 \times 0.25^\circ$  resolution along latitude and longitude and in the monthly mean from 1979-2016 (Dee *et al.*, 2011). Then, the wind stress ( $\tau$ ) was calculated on the surface of the ocean via:

$$\tau = \rho_a C_d V \quad (1)$$

where  $\rho_a$  represents air density (equal to  $1.22 \text{ kg/m}^3$ ),  $C_d$  represents drag coefficient, equal to 0.0013 without unit (Sengupta *et al.*, 2001), and  $V = \sqrt{u^2 + v^2}$  shows the magnitude of the wind vector. Therefore,  $\tau$  was calculated, in the monthly mean of 1979-2016, in  $0.25 \times 0.25^\circ$  resolution.

In this study, to investigate the leading spatial and temporal pattern of the sea level anomaly, surface net heat flux and wind stress, the method of the principal component analysis was employed, often referred to as the Empirical Orthogonal Function (EOF) analysis. This method finds spatial patterns (modes) of variability and corresponding their time variation, obtained by

the expansion coefficients of spatial patterns, that represents the temporal variations of the leading EOF pattern (time series of EOFs or time series of principal component). Subsequently, a spectral analysis was performed using the Fast Fourier Transform (FFT) technique on the time series of EOFs, for determining the dominant frequencies. As a second step, the correlation analysis was applied to the time series of EOFs. The purpose was to investigate the interactions of the dominant temporal patterns of each quantities of net surface heat flux and wind stress separately (irrespective of other effective factors) relative to the sea level anomaly in NWIO. With this assumption, the relationship between these two quantities with the sea level can be considered linear. Therefore, the correlation analysis will be usable in accordance with researches such as Li and Han (2015) and Dhage and Strub (2016).

In the third step, considering all components of the sea level change are not dynamic in nature, the study of inverted barometer effect was assessed. The inverse barometer effect is the most important. As explained in the introduction, sea level signal processing may not be as expected to detect this component. Thus, inverted barometer effect was directly calculated by using the physical relations and required quantity data. To calculate the inverted barometer effect, the total sea level anomaly  $\eta_{tot}$  can be taken as:

$$\eta_{tot} = \eta_{ib} + \eta_r \quad (2)$$

where  $\eta_{ib}$  represents a part of the anomaly resulting merely from the inverted barometer effect, and  $\eta_r$  is the non-barometric effects resulting from other constructive processes of the sea level anomalies, including the steric changes and the barotropic effect on the sea level (Piecuch *et al.*, 2016a).  $\eta_{ib}$  can be taken as:

$$\eta_{ib} = -\frac{P_a - \overline{P_a}}{\rho_{ss} g} \quad (3)$$

where  $P_a$  represents the barometric pressure,  $\rho_{ss}$  is sea surface density and  $g = 9.81 \text{ ms}^{-2}$  represents the acceleration of gravity.

Density is a function of pressure, temperature and salinity. Therefore, in order to calculate  $\rho_{ss}$ , sea level pressure (SLP), sea surface temperature (SST), and sea surface salinity (SSS) are needed. In the present study, SLP, SST and SSS were obtained from ECMWF, OISST2 (Optimum Interpolation Sea Surface Temperature) and AQUARIUS, respectively. The SSS data is limited to parts of NWIO in the Arabian Sea and not available in other neighboring regions.

After compiling the required data using the Thermodynamic Equation of Seawater 2010 (TEOS-10) which realises a fairly accurate estimation of parameters, such as density and specific volume, based on the Gibbs-Helmholtz equation, the sea surface density was calculated (McDougall *et al.*, 2003; Roquet *et al.*, 2015). With regard to the availability of SSS data for 36 months, sea surface density (2012-2015), was calculated as monthly mean. As a result,  $\rho_{ss}$  and then  $\eta_{ib}$  were calculated for a three-year annual cycle. Then, the total sea level anomaly difference from its inverted barometer component was considered with the subtraction of  $\eta_{ib}$  from  $\eta_{tot}$  in order that the inverted barometer effect on the sea level in the study area can be found and the spatial distribution of  $\eta_{ib}$  and  $\eta_r$  can be investigated. Due to the lack of long-term effects of barometer pressure on long-term sea level changes, a study conducted in a three-year period can be useful for evaluating the inverted barometer effect in the region.



### 3. Results

#### 3.1. Trend

Fig. 1 shows the spatial distribution of the sea level trend, related to the sea level anomaly data used in this study. As this figure illustrates, the sea level trend is positive over whole the Arabian Sea, except in very limited regions where it is negative. The trend in sea level height varies from -1.5 to +8.5 mm/year throughout the region, although it is mostly positive. In addition, it reaches its maximum in some parts of west coast of India. It has been known that altimeter near coastal region is not reliable. The highest signal in regions of 22° N, 74° E might be noise.

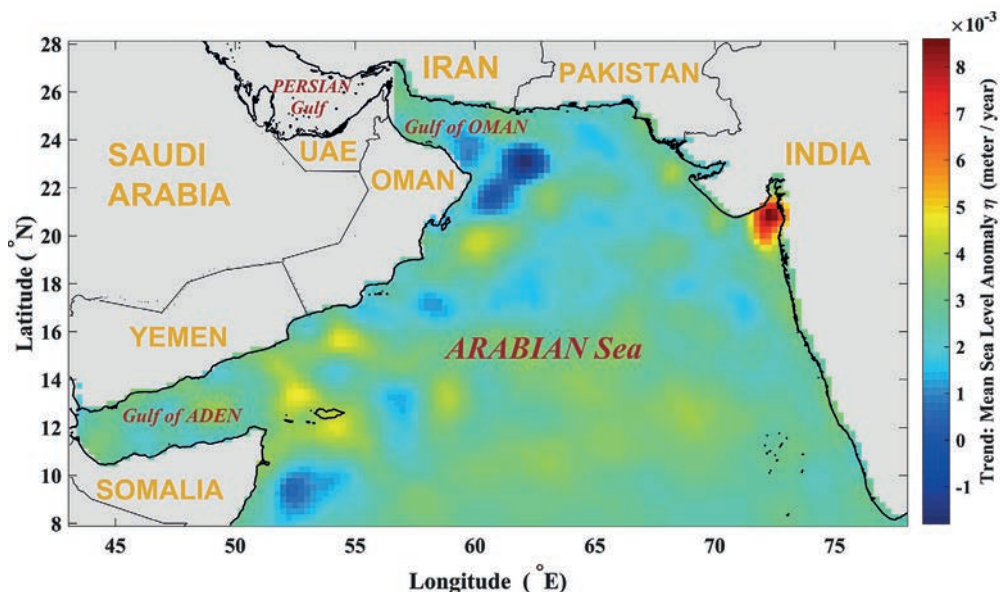


Fig. 1- NWIO sea level trend calculated for the period 1993-2015.

In general, the results obtained from the application of the trend analysis on the data used in this study are consistent with those of previous studies, such as Church *et al.* (2004), Unnikrishnan *et al.* (2006), Unnikrishnan and Shankar (2007), and Han *et al.* (2010), which indicated positive trends in sea level in most parts of the northern Indian Ocean using in situ and satellite data as well as climate simulation models. Moreover, the results were consistent with those of Parekh *et al.* (2017) which used the analysis of the linear trend of the northern Indian Ocean in the time period 1995-2008 and stated that the rising trends of sea level were higher in the Bay of Bengal than in the Arabian Sea. Therefore, the negative trends should be reported in some parts of Arabian Sea. As shown in Fig. 1, the trend in sea level anomaly is negative in some parts of the western and north-western regions of the Arabian Sea, but it is positive in other parts of NWIO. In accordance to above results and the accuracy of the data, other objectives of the study can be assessed.

#### 3.2. EOF, spectral and correlation analysis

Fig. 2 illustrates the four leading EOF patterns of sea level anomalies. These modes together account for 99.7% of the total sea level anomalies variance. Sea level changes show spatially

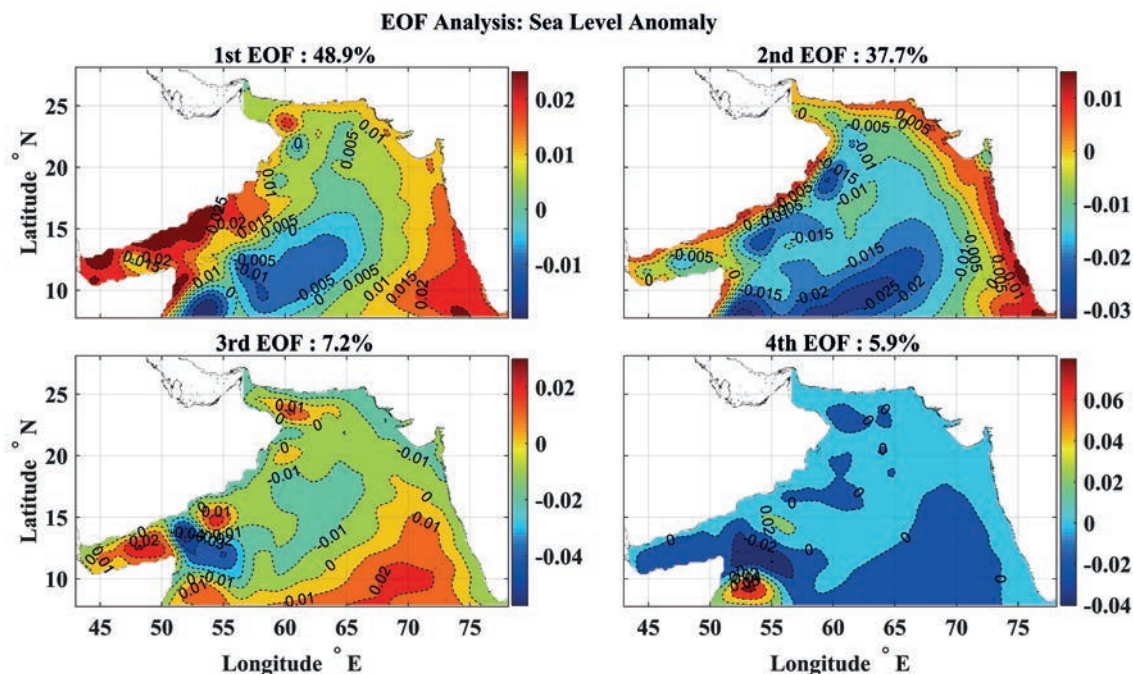


Fig. 2 - Spatial patterns of the four EOF modes of sea level anomaly.

very different patterns and sea level rises in different parts of the study area are associated with different modes.

The 1st EOF shows the seasonal variability of the study area with the predominant spatial distribution of positive anomalies and the 2nd EOF is related to El-Nino and the positive phase of IOD that cause negative anomalies in the sea level by the exacerbated warming and evaporation (Du *et al.*, 2009; Soumya *et al.*, 2015; Parekh *et al.*, 2017). Therefore, the second pattern of changes in sea level (2nd EOF with a low percentage of eigenvectors compared to the 1st EOF) shows the effect of these two natural events on the formation of anomalies. In addition, in most of the leading EOFs the sea level anomalies, especially the 1st and 2nd EOFs, are noticeably positive in the area along the coast. As moving off the coast, contours appear to be negative. This indicates that the coastline has caused the sea level rise relative to the mean value due to the effects of coastal Kelvin waves (Hendon *et al.*, 1998). In the Indian Ocean, during monsoon, equatorial winds drive equatorial downwelling Kelvin waves which radiate westwards moving Rossby waves. Propagation of planetary Kelvin and Rossby waves can be observed using sea surface anomaly. The equatorial Kelvin waves, as they reach the coast, reflect as coastal Kelvin waves (Gera *et al.*, 2016). The 3rd EOF, with an approximately equal distribution of positive and negative anomalies, shows that the maximum sea level anomalies are located in the Gulf of Aden, and the 4th EOF with the least percentage of eigenvectors shows the distribution of negative anomalies with the minimum expanded at about 50-55° E. In general, examining the four leading EOF modes of sea level anomalies, the maximum sea level change is greater in the areas adjacent to Gulf of Aden and its minimum is in the centre of the ocean, near the equator and towards the SW.

Fig. 3 shows the time series of principal component of the first four EOF modes of sea level anomalies (left panels), obtained by the expansion coefficients of spatial patterns, and the

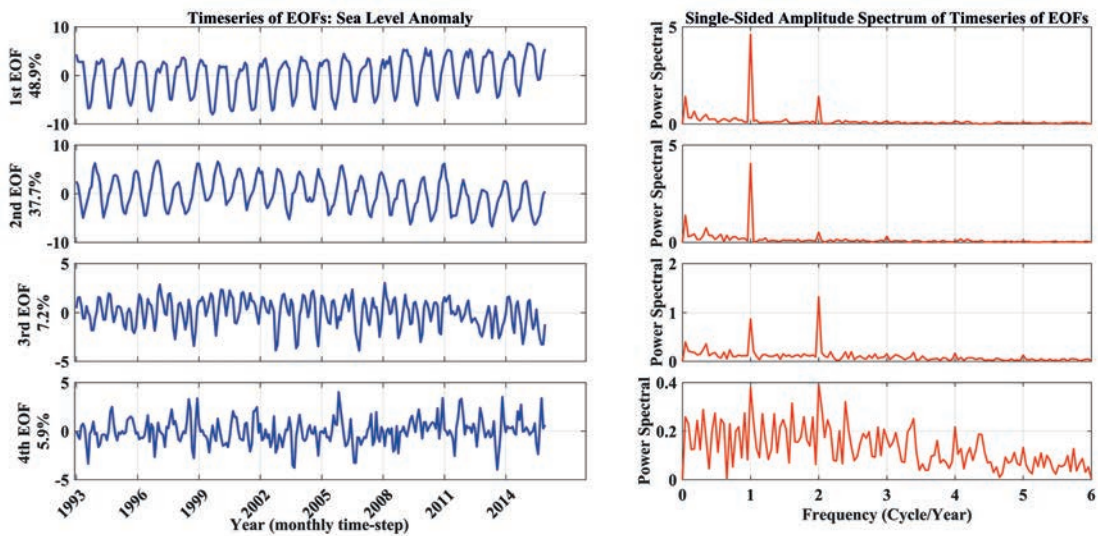


Fig. 3 - Time series of expansion coefficients and spectra of the four EOF modes of sea level anomaly.

results of applying spectral analysis using the FFT technique on the time series of EOFs (right panels).

In general, the 1st and the 2nd EOF modes which accounts for 48.9% and 37.75% of the variance, respectively, are close to each other and both of them account for less than 50% of the total variance, so 1st and 2nd EOF are very similar in terms of power spectra and time series of the expansion coefficients. The results obtained from spectral analysis show an expected behaviour for the mean sea level: the 1st EOF has the greatest power among the four leading EOF modes for low frequencies. According to the results, the time series of the 1st and 2nd EOFs have a dominant annual frequency. Consequently, the main causes of sea level changes in NWIO are weakened and intensified with a one-year period, while the time series of the third factor affecting sea level changes, obtained from the EOF analysis, strengthened and weakened with a six-month period. In fact, 3rd EOF mode which accounts for 7.2% of the variance, is considered as the resultant of the effects that takes place twice a year in NWIO such as monsoonal effects and some other local climatic factors. In the higher modes, the spectral power amplitude is constantly reduced so that it reaches a very small and irregular amount in the 4th EOF. Therefore, low power spectrum, irregularity of the power spectrum in terms of frequency, severe and irregular changes in the time series, and the lower contribution of this mode to the total variance, show the low significance of this mode in general surveys of the sea level anomalies. Generally, apart from the 4th EOF, which indicates irregular and random variations over time intervals, other time components are replicable in nature due to their periodic variations. Fig. 4 illustrates four leading EOF patterns of net surface heat flux anomalies accounting for 99.8% of the total surface net heat flux variance.

Fig. 4 shows the most leading mode of surface heat flux in NWIO (1st EOF), as a basin-wide, in a uniform and homogeneous form with negative anomalies. In the first place, this means that heat is predominantly transferred from NWIO to the atmosphere. In addition, the negative sign in Fig. 4 can be strengthened by the increasing effects of surface winds and an increase in cloud coverage over the ocean surface heat flux. In this mode, there are signs of the effects of ENSO. Previous studies have also shown that the ENSO index, as high correlation, results in



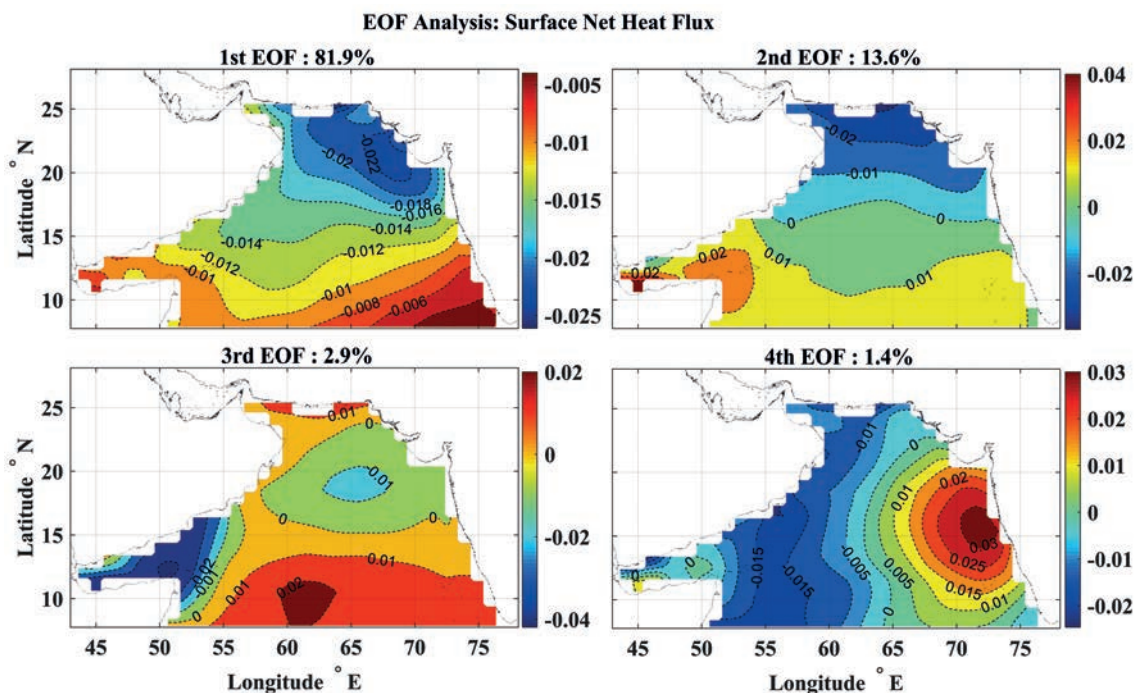


Fig. 4 - Spatial patterns of the four EOF modes of surface heat flux.

the formation of a basin-wide and uniform temperature (Yamagata *et al.*, 2004), and surface heat flux is known as the main cause of SST changes in the ENSO causing temporal changes of thermocline height (Venzke *et al.*, 2000; Deser *et al.*, 2010; Wu *et al.*, 2017). According to Fig. 4, the 2nd EOF distinguishes between north and south areas of the region with zero counter. The northern region includes the Gulf of Oman and the coasts of India with negative anomalies, and the southern region is near the equator with positive thermal anomalies. In other words, the 2nd EOF mode of surface heat flux anomaly is the N-S dipole mode so as the positive/negative phase of the dipole mode is observed in the southern/northern region. The increase in the severity of surface winds in the northern Indian Ocean enhances the process of evaporation and loss of surface heat through turbulence of heat flux (Murtugudde *et al.*, 2000). In the southern parts of NWIO, near the equator, positive heat flux is observed due to the decrease in surface wind speed. So, the 2nd EOF was considered as a mode from the internal effects of the northern Indian Ocean on the heat flux.

The 3rd and 4th EOFs of surface heat flux observed in Fig. 4 are less important in the discussion due to the small contribution to the variance of the surface heat flux of the region.

Fig. 5 shows time series of expansion coefficients and the dominant power spectrum of 1st to 4th EOF modes of surface heat flux anomalies. The oscillatory movement in the mentioned time series is a periodic change that has been caused by the ups and downs of sea level in a long-term period. Moreover, because of the oscillation of surface heat flux around a fixed horizontal axis, the stationary time series is observed in the mean. The results obtained from spectral analysis show a significant power with the frequency of an annual cycle. This power belongs to the 1st and 2nd EOFs. Other components affecting the surface heat flux with two cycle/year frequency for the two leading modes (1st and 2nd EOFs) are considered. This is due to the small difference of

power spectrum compared to the maximum power. This dominant peak of the frequency is also observed in the 3rd and 4th EOFs. Also, a three cycle/year is recognisable from the 3rd EOF power spectrum. These prove that the components affecting the NWIO surface heat flux are complex and they are not limited to known factors. These results were reported in previous works. For example, Clemens *et al.* (1991) stated about the western Arabian Sea vertical processes, as well as horizontal advection, contribute significantly to SST interannual variability, and the wind is not the only factor controlling the heat flux forcing. Also, unusual climatic conditions with different forms and scales sometimes occur in the area (Behera *et al.*, 1999). However, the effects of powerful, encompassing and sequential phenomena such as monsoon, IOD and ENSO on the surface heat flux will be greater than other possible factors. Therefore, according to the results obtained from Fig. 4 and a logic-based inference, the semi-annual cycle of NWIO surface heat flux is dominant rather than the annual cycle, and it is likely that the monsoon is a strong influence in NWIO and this result correlates with the power spectrum of 3th EOF mode of sea level anomaly in Fig. 3.

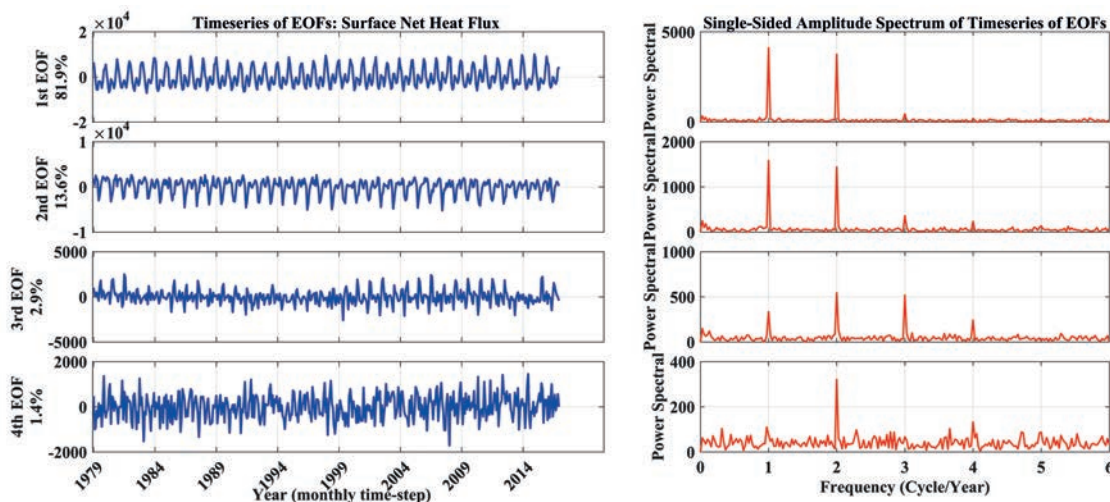


Fig. 5 - Time series of expansion coefficients and spectra of the four EOF modes of surface net heat flux.

So, with a general view of all four EOFs, the most dominant peak of power spectrum of the surface heat flux can be considered in the six-month peak area and its dominant changes are seasonal. The four leading EOF modes of wind stress, accounting for 99.8% of the total wind stress variance, are as shown in Fig. 6. The 1st EOF of wind stress, with the eigenvalue as 95%, is the most leading EOF for wind stress anomalies, which is a uniform mode with all negative counters whose value becomes less negative as moves towards the north. In the case of a negative sign it can be stated that the wind stress results in a transfer of horizontal momentum between the air and the sea by the vertical momentum flux. Wind stress magnitude is numerically equal to the magnitude of the momentum flux. For this reason, it is a common practice not to differentiate between stress and momentum flux. By convention, the momentum flux is defined to be positive downwards (from atmosphere to ocean). In this case, waves extract momentum from the wind. Negative momentum flux corresponds to upward momentum transfer (from ocean to atmosphere). This regime is associated with the wave-driven wind (Grachev *et al.*, 2003).

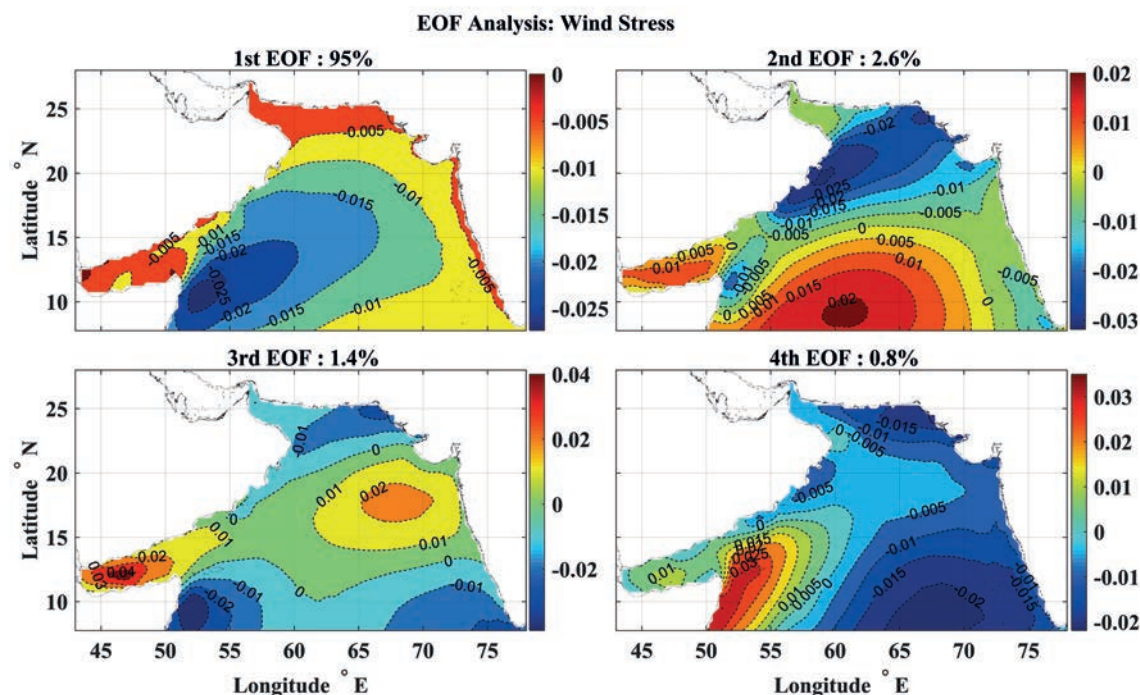


Fig. 6 - Spatial patterns of the four EOF modes of wind stress.

The entire northern Indian Ocean is surrounded by monsoonal and seasonal winds hitting the equator. The most leading spatial patterns of wind stress indicate that the anomalies of north-eastern winds blow toward the Arabian Sea and along the equator toward the coasts of Africa in the SW of the region. This justification was obtained earlier in Schott *et al.* (2009).

Fig. 7 shows the time series of principal component and power spectrum corresponding to the four leading EOF modes of wind stress. The oscillatory movement in the time series of expansion coefficients of the 1st EOF is considered to be the most leading mode of systematic, regular, and annual variations with natural repeatability that has been created due to the ups and downs of a long-term period. According to this chart, the wind stress has reached its minimum for certain cases in a limited range while the regular fluctuations are observed in other ranges in time components.

The dominant peak of the time series of 1st EOF indicates that the dominant wind stress changes applied to NWIO oscillate with an annual cycle frequency. Therefore, the period of wind stress changes is due to the common annual variations in climatic condition of NWIO corresponding to the one-year period sea level anomalies, but the range of power spectrum of wind stress is more intense, than sea level anomaly. However, the next influential frequency in this mode is 2 cycle/year. In particular, it can indicate the effect of monsoon on the wind system of NWIO. In the 2nd EOF, suddenly, power spectrum reduces significantly so that the power spectrum of the highest peak in this mode is about a tenth of power spectrum of the 1st EOF. This decrease in power spectrum amplitude continues in other modes in such a way that it is very small in the 4th mode. This issue is predictable due to the small contribution that the 2nd to 4th EOFs of wind stress anomalies have from the total variance, and makes the insignificant effect of these modes on the changes in the region's wind stresses more clearly.



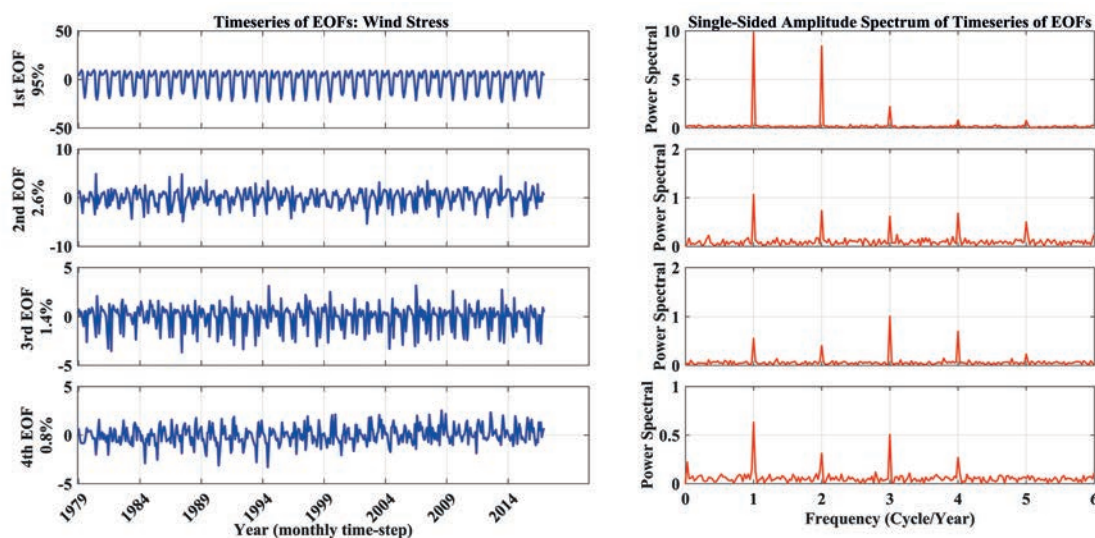


Fig. 7 - Time series of expansion coefficients and spectra of the four EOF modes of wind stress.

After examining the temporal and spatial components of the quantitative factors affecting the formation of sea level anomalies via the EOF and spectral analyses, now using the correlation analysis, the strength and intensity of the relationship between these quantities and the sea level are investigated to identify the most prominent interactions leading to the formation of sea level anomalies in NWIO.

The results of this analysis are summarised in Table 1, showing the cross-correlation coefficients obtained between the time series of the four discussed surface heat flux, wind stress modes, and the time series of the four sea level anomalies modes. Considering Table 1, the correlation coefficients of the two values of heat flux and wind stress with the 2nd EOF of the sea level are higher than any other modes. This means that the 2nd EOF of the sea level with 37% of the total variance is a dominant one which is mostly affected by physical quantities such as wind stress and heat flux which are affected by climate changes and dynamics of ocean.

In the upper half of Table 1, most of the correlation coefficients between the modes of sea level anomalies and surface heat flux are positive when the correlation between them is significant ( $p$ -value lower than 0.05). This means that, in accordance with expectations in NWIO, the correlation between the surface heat flux and the sea level anomaly is direct, and the increase in the flux of heat is accompanied by an increase in the regional sea level. It has already been concluded that both of these modes include the effects of factors outside the Indian Ocean (external factors) on the heat flux such as ENSO. Therefore, external factors have a profound effect on the changes in the physical quantities of NWIO. However, the correlation coefficient between the leading modes of EOFs of these two quantities is 0.151. That means, the leading pattern of sea level anomaly will be less driven by variations of surface heat flux in NWIO. Moreover, the coefficients obtained between the 2nd EOF of surface heat flux and the 1st and 2nd EOFs of the sea level are significant. Previously, the 2nd EOF of surface heat flux, which had a relatively lower percentage of the variance of heat flux data, was considered as a mode from the internal effects of the northern Indian Ocean on the heat flux. According to the results obtained from the correlation analysis, it can be concluded that the effects of internal factors are lower than those

of external factors, but it was not affected by sea level anomalies, and despite its low intensity (13.6% vs 81.9%), it has a similar effect on sea level anomalies in terms of behaviour on sea level anomalies of NWIO.

Table 1 - Results of correlation analysis between time series of EOFs.

Correlation Analysis <i>r</i> : Correlation Coefficient [-1,1] <i>p</i> : P-Value		Sea Level Anomaly			
		1st EOF: 48.9%	2nd EOF: 37.7%	3rd EOF: 7.2%	4th EOF: 5.9%
Surface Heat Flux	1st EOF: 81.9%	$r = 0.151$ $p = 0.011$	$r = 0.639$ $p = 10^{-33}$	$r = -0.091$ $p = 0.133$	$r = 0.119$ $p = 0.049$
	2nd EOF: 13.6%	$r = 0.227$ $p = 10^{-4}$	$r = 0.528$ $p = 10^{-21}$	$r = -0.014$ $p = 0.811$	$r = 0.025$ $p = 0.681$
	3rd EOF: 2.9%	$r = -0.390$ $p = 10^{-11}$	$r = 0.029$ $p = 0.635$	$r = 0.33$ $p = 10^{-8}$	$r = -0.158$ $p = 0.008$
	4th EOF: 1.4%	$r = 0.291$ $p = 10^{-7}$	$r = -0.134$ $p = 0.027$	$r = -0.268$ $p = 10^{-6}$	$r = -0.017$ $p = 0.781$
Wind Stress	1st EOF: 95.0%	$r = 0.485$ $p = 10^{-17}$	$r = 0.452$ $p = 10^{-15}$	$r = -0.205$ $p = 10^{-4}$	$r = 0.106$ $p = 0.07$
	2nd EOF: 2.6%	$r = 0.129$ $p = 0.033$	$r = 0.471$ $p = 10^{-16}$	$r = -0.058$ $p = 0.336$	$r = 0.146$ $p = 0.015$
	3rd EOF: 1.4 %	$r = 0.052$ $p = 0.383$	$r = 0.318$ $p = 10^{-8}$	$r = 0.166$ $p = 0.005$	$r = -0.107$ $p = 0.07$
	4th EOF: 0.8 %	$r = -0.272$ $p = 10^{-6}$	$r = 0.166$ $p = 0.005$	$r = -0.108$ $p = 0.07$	$r = 0.057$ $p = 0.34$

Regarding the coefficients obtained between the time series of the EOFs of sea level anomalies and wind stress and the occurrence of the majority of positive (direct) correlation coefficients, especially in leading modes, it can be concluded that the wind mode and the effects of wind stress on the waters of NWIO are often such that Ekman pumping pumps warm water towards the bottom of the ocean (downwards) and causes positive regional sea level anomalies with increasing tropical thermocline. The first EOF of wind stress, with a significant percentage of the total variance, has significant correlation coefficients as 0.485 and 0.452, respectively, with each of the two 1st and 2nd EOFs of sea level. In addition, the correlation coefficient between the 1st EOF of wind stress and the 3rd EOF of mean sea level anomaly, which has a relatively small share of the variance of its values, is as -0.205. The negative sign indicates the reverse effect of wind stress on this EOF of sea level. Considering the significance of this negative correlation coefficient, it can be attributed to the relative frequency of Ekman suction and the upwelling phenomenon in NWIO basin. However, the correlation coefficient (0.205) is significantly lower than the sum of positive significant coefficients obtained between the 1st EOF of wind stress and the 1st and 2nd EOFs of the sea level (0.485 + 0.452). As a result, the wind-driven upwelling that is partly on the coastal and NWIO with relatively intermittent patterns, are very scattered and few compared to the entire surface of this region. There are also significant correlations with considerable coefficients between the other modes of wind stress and sea level anomalies. But because of the insignificant contribution of these modes, the variance of the wind stress values is considered insignificant; thus, only their values are indicated in Table 1.



### 3.3. Inverted barometer effect

Figs. 8 and 9 show the meridional distributions of zonal mean and for 12 months, respectively. As illustrated in these figures,  $\eta_{ib}$  decreases in autumn and winter as well as by moving towards the high latitudes, while it increases in high latitudes during spring and summer. Maximum and minimum values of  $\eta_{ib}$  are created in July. The maximum value (+0.069 m) is related to the highest latitude of the region at about 24° N and its minimum (-0.048 m) at the lowest latitude of about 8° N. Changes in the inverted barometer effect around 14° N (mid-latitude of the Arabian Sea) are negligible. In other words, in this latitude band, the inverted barometer does not have a significant effect on the overall sea level anomaly. But it would be effective with moving to higher or lower latitudes. By examining the graphs obtained in Fig. 8 it can be inferred that the inverted barometer effects on the sea level anomalies in the Arabian Sea variate with two parts in a year (seasonally). This oscillation is mirrored from high to low latitudes. It means that by moving from the high latitudes, the inverted barometer effect results in the sea level rise, and by moving towards low latitudes, the rate of this bulge decreases gradually and becomes a concavity in the mid-latitude of the Arabian Sea, so that the concavity depth is increased up to 8° N latitudes (or vice versa). In general, in the Arabian Sea, the tendency towards a concavity/bulge of the sea level caused by the inverted barometer in the low/high latitudes is greater than the high/low latitudes. With the start of the year in January, the inverted barometer effect on the sea level increases from the high to low latitudes and gradually the tendency of effectiveness reduces until April when the tendency of effectiveness changes along latitude. As the inverted barometer effect reduces with the reduction in the latitude, the intensity of its effectiveness increases until July. After August, the intensity of its effect decreases until October when it reaches its lowest amount, and then again in November and December, towards the spring, the trend changes along the latitude so that with the reduction in the latitude, the inverted barometer effect on sea level results in the sea level change (bulge) and the intensity of the inverted barometer effect will increase (more positive anomalies).

According to Fig. 9,  $\eta_{tot}$  has irregular fluctuations in different latitudes, due to the influence of several factors. But it is clear that, the latitudinal mean of  $\eta_{tot}$  in all over the Arabian Sea has

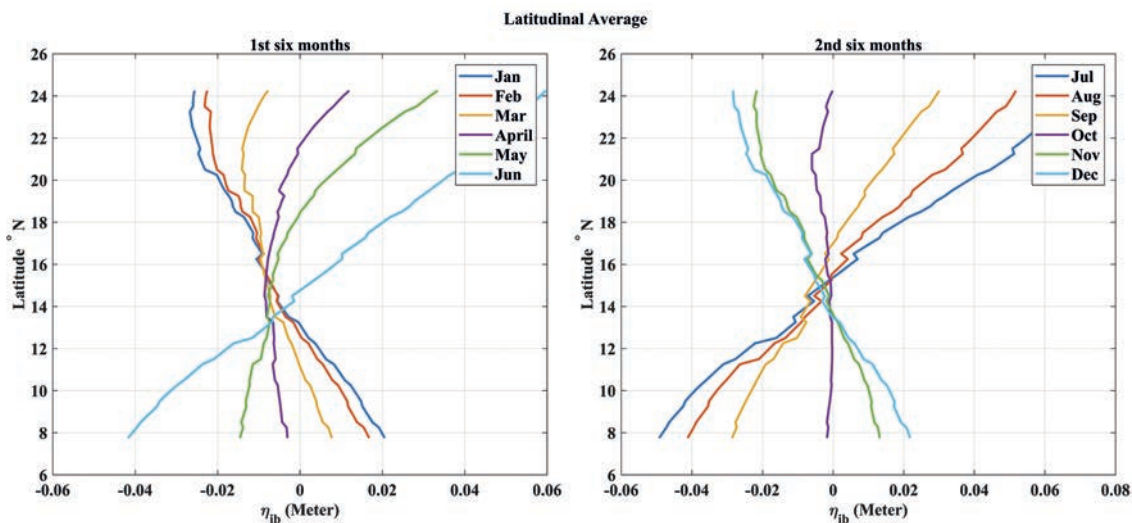


Fig. 8 - Latitudinal mean of  $\eta_{ib}$ .

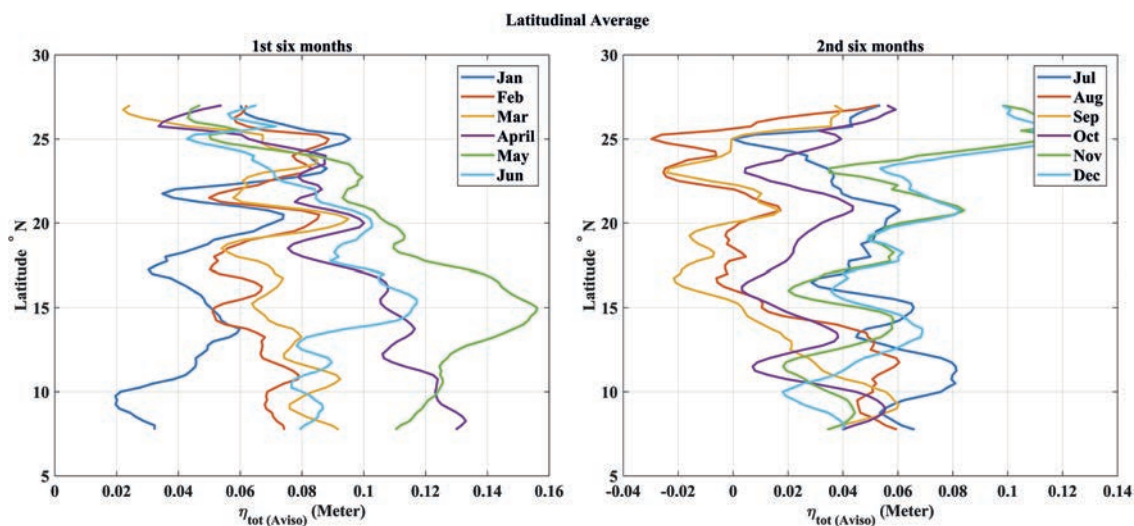


Fig. 9 - Latitudinal mean of  $\eta_{tot}$ .

positive anomalies over most months, except in August and September at higher latitudes. This indicates a sea level change in most parts of the region.

The maximum latitudinal mean of  $\eta_{tot}$  is in May and around  $14^{\circ}$  N (+0.152 m) and its minimum is formed in September and around  $16^{\circ}$  N (-0.013 m). In the first six months of the year, the sea level anomaly differences in the high latitudes are very low, and the graphs in the higher latitudes converge to a certain number of anomalies, but with the reduction in the latitude, the sea level anomaly differences in each month of the first half of the year has risen, and these differences are remarkably significant at the lowest latitudes. This process is reversed in the second half of the year. Indeed, the values of the sea level anomalies are closely aligned with the lower latitudes and are dispersed into different values of sea level anomalies by the increase in latitudes.

Comparing the corresponding months in Figs. 8 and 9, it appears that in general, in months of the second half of the year, sea level anomalies, especially in the high latitudes of the Arabian Sea, are associated with significant positive amounts (November and December), and the inverted barometer effect in higher latitudes leads to a negative sea level anomaly. In fact, it can be concluded that at the onset of winter monsoons, when the influence of the Southern Oscillation Index still dominates the climate conditions of the Arabian Sea (Shukla, 1987b; Webster *et al.*, 1998; Church *et al.*, 2006), the ocean's sea level will be so much affected by the dynamic components that the inverted barometer does not play a significant role in  $\eta_{tot}$ . In the first six months of the year, when sea level anomalies, especially in the lower latitudes of the Arabian Sea (significantly in April and May) are positive, the intensity of the inverted barometer effect is not high, and its changes along the latitude are not significant. But in other months, we can see the significant inverted barometer effect on  $\eta_{tot}$ .

For a clearer distinction, the annual cycles of the distribution of the inverted barometer effect  $\eta_{ib}$  and other signals affecting the global sea level  $\eta_r$  ( $\eta_r = \eta_{tot} - \eta_{ib}$ ) in the Arabian Sea are obtained. Figs. 10a and 10b illustrate the mean annual cycle calculated for the period 2012-2015. For most months,  $\eta_{ib}$  appears as diagonal stripes stretching from NE to SW. This trend is different in months of the year, especially in April and October, at the beginning of seasonal changes (from

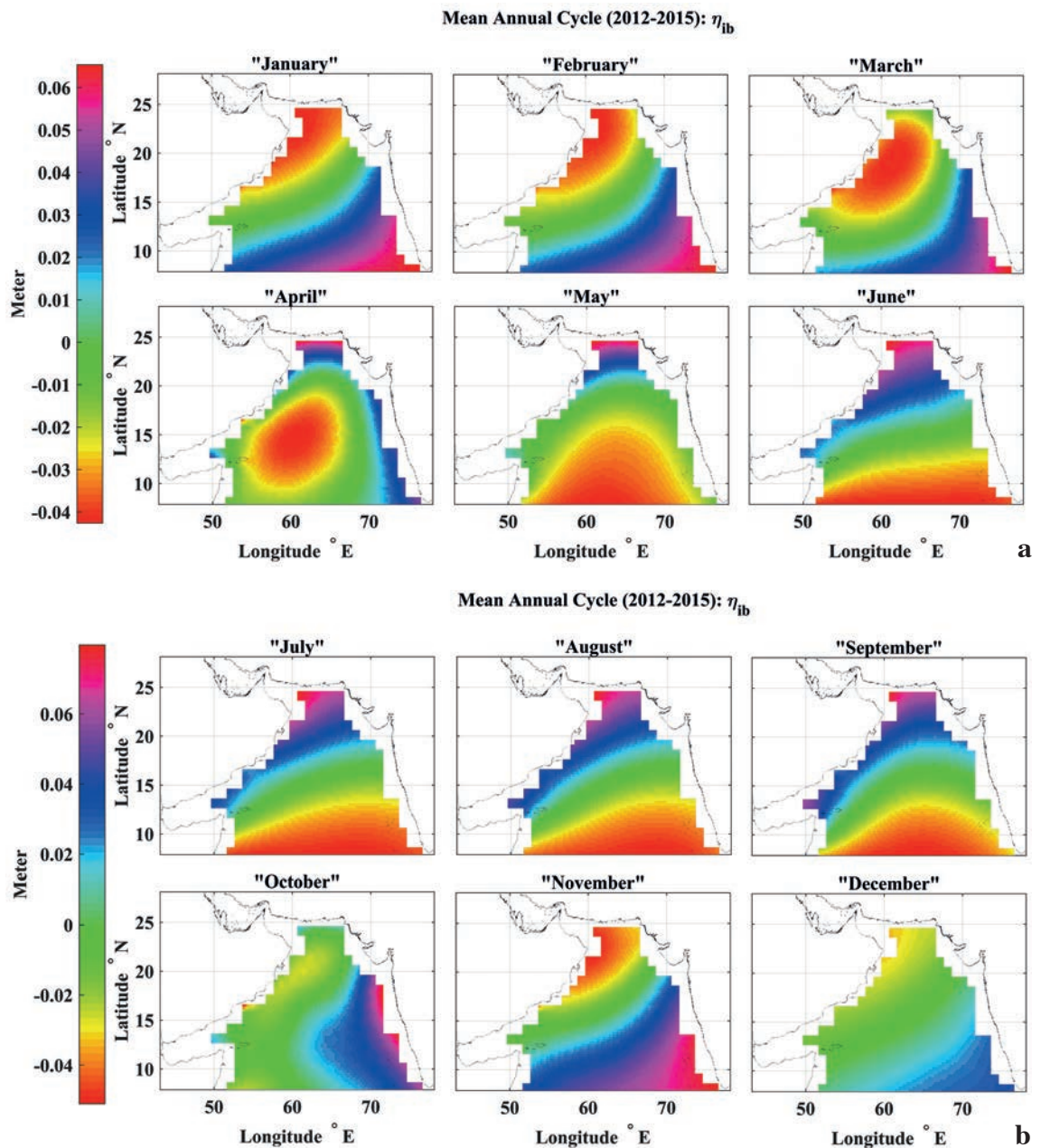


Fig. 10 - Annual cycle of  $\eta_{ib}$ : a) first six months; b) second six months 2012-2015.

winter to spring and from summer to autumn). During the two winter months of January and February, aggregations of positive  $\eta_{ib}$ s have been observed in low latitudes extending throughout the longitude of the region, so in these areas the inverted barometer effect will cause the sea level to rise, and the maximum of the sea level anomaly is observed in the south-eastern Arabian Sea. As moving towards the Gulf of Oman, negative  $\eta_{ib}$ s appear and extend in the central regions of the Arabian Sea on diagonal stripes extending from the east to the Gulf of Aden, the inverted barometer will not have a significant effect on sea level anomalies.

In March, approaching the spring, the sea level in the northern areas of the Arabian Sea and adjacent to the Gulf of Oman tends to positive  $\eta_{ib}$ s, but the maximum of  $\eta_{ib}$ s (about 0.06 m) along the latitude and longitude of the area are less seen. In April, the minimum  $\eta_{ib}$  is seen in the central regions of the area, so as by moving towards the coasts, its value increases and the maximum value is observed in the northern Arabian Sea. In spring and summer months (May to September), locations of maximum  $\eta_{ib}$ s are completely different from winter months so that the highest inverted barometric effect causing the sea level rise, is located in the northernmost region of the Arabian Sea. In October, by moving from the east to the west along the longitude,  $\eta_{ib}$  values reduce, so maximum  $\eta_{ib}$  is seen in the eastern regions and its minimum is observed in the western regions. On this basis, the  $\eta_{ib}$  distribution formation of the Arabian Sea continues in the fall months, which gradually the effect of  $\eta_{ib}$  decreases by the end of December, and the maximum and minimum values  $\eta_{ib}$  of this month are smaller than in other months.

Naturally, the monthly mean of  $\eta_r$ , which is the sum of other factors affecting  $\eta_{tot}$ , are separately illustrated in Fig. 11. They have irregular spatial oscillations and positive, negative, and zero values in different latitudes. The range of positive  $\eta_r$ s across the area and all the months is greater than negative values. This indicates that factors such as barotropic and steric changes tend to rise the sea level of the Arabian Sea. In winter months as approaching the spring, the effect on the sea level reduces, although in the south-western sub-regions, near the coast of India as well as the adjacent areas of the Gulf of Aden, there are significant positive effects. The northern Arabian Sea in the adjacency of the Gulf of Oman in the third quarter of spring, especially in the month of May have negative values of  $\eta_r$  term so that this negative effect continues in the summer months. It is also observed that the effect of non-barometer factors on the sea level in these areas is greater than the lower latitudes. During these months, the  $\eta_r$  value has increased to a large extent in the southern Arabian Sea area (an area which connects the Arabian Sea to ocean).

It can be observed that with the onset of the spring, the interaction effect of the Indian Ocean's waters with the Arabian Sea results in the sea level rise by the end of the summer in a form that does not have a barometric nature and can be considered as barotropic or steric, due to mixing of the Indian Ocean waters with the Arabian Sea is induced to the sea level. Moreover,  $\eta_r$  as a component outside of the inverted barometer effect, can mainly involve the steric effect caused by thermal expansion and salinity; therefore, it is expected that during summer months, the effect of this component will be maximised with the increase in temperature and evaporation. With the end of summer, the non-barometric effect of the southern Arabian Sea will be moved to the west and NW. In addition, its value will decrease until in December (the last month of the fall), the effect of  $\eta_r$  on the creation of sea level anomalies of the Arabian Sea, particularly in its central parts, reaches its lowest point of the creation. At the onset of the winter, it resumes its increasing trend in scattered parts of the Arabian Sea, especially in areas near the coasts.

In total, alternation and periodicity of fluctuation as a quasi-static component of sea level anomaly reveal the importance of  $\eta_{ib}$  impacts of this type of components on NWIO sea level fluctuations. On the other hand, with an assumption that the most considerable aspect of sea level changes is related to the inverted barometer effect, the  $\eta_r$  can be considered as an index for total dynamic changes in sea level height. Also, according to the evidence obtained in this study, the magnitude of  $\eta_{ib}$  is less than  $\eta_r$  across the NWIO. So, the periodic pattern of variation in sea level anomaly with less contribution in data variance, that was introduced as the 3rd EOF with 7.2%, can demonstrate the quasi-static sea level changes in the NWIO.



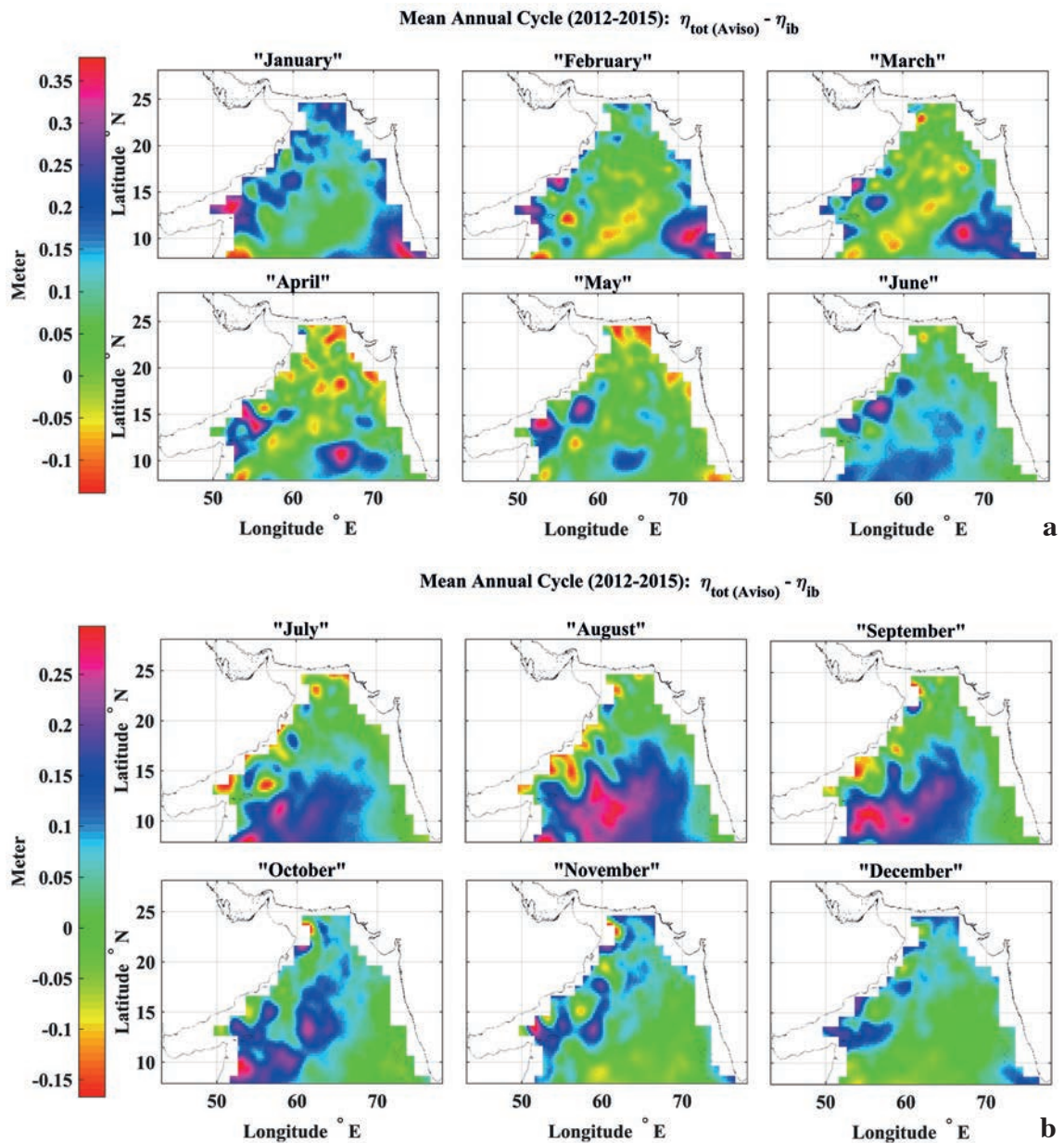


Fig. 11 - Annual cycle of  $\eta_r$ ; a) first six months; b) second six months 2012-2015.

#### 4. Conclusion

The sea level changes in NWIO Ocean were analysed from different perspectives. Basically, the processes affecting regional sea level changes can be divided into dynamic (such as the effects of surface heat flux and wind stress on the sea level fluctuation) and quasi-static components (such as inverted barometer effects). First, the temporal trend in mean sea level anomalies was determined. Second, by using EOF, the leading spatio-temporal patterns of mean sea level anomaly, net surface heat flux and wind stress were found and the results were compared. These can, in



some way, overwhelm the dynamical variabilities of the sea level height and cause significant changes in sea level on the interannual to interdecadal time-scale. In addition, they may affect the long-term trend. Then, using spectral analysis and time series, the temporal cycles of the dominant changes in these three quantities were investigated. Also, the correlations between the time series of EOFs were evaluated to realise the effect of these two quantities on the sea level anomalies in the region. Third, focusing on the inverted barometer effect, contribution of quasi-static component of sea level anomaly was determined and the annual cycles of this effect were obtained. According to the results:

- the spatial distribution of positive eigenvectors in the 1st EOF of sea level anomalies (48.9%) indicates a sea level fluctuation which highlights the effects of seasonal sea level change. However, in the 2nd EOF (37.7%), the effects of regional factors such as the ENSO and the IOD are obvious. As a result, these two EOF modes can be attributed to the dynamic changes in NWIO sea level anomaly. In general, examining the four leading EOF modes of sea level anomalies, the maximum sea level change is greater in the areas adjacent to Gulf of Aden and its minimum is in the centre of the ocean, near the equator and towards the SW;
- the maximum correlation coefficient between the 1st EOF of heat flux anomalies and the 2nd EOF of the sea level anomaly is equal to 0.639. It has already been concluded that both of these modes reveal the effects of factors outside the Indian Ocean on the surface heat flux, such as the ENSO. As a result, ENSO has a profound effect on the surface heat flux and consequently on the sea level anomalies in NWIO. Also, according to the correlation results between the time series of EOFs of sea level anomalies and wind stress, effects of wind stress on the waters of NWIO are often such that Ekman pumping pumps warm water towards the bottom of the ocean (downwards) and causes positive regional sea level anomalies with increasing tropical thermocline. So, the upwelling is far more than downwelling occurs in NWIO;
- commonly, the dependence of the inverted barometer effect on the latitude is very significant in the region. By moving to the high/low latitudes, the inverted barometer effect decreases/increases in the cold months/warm months. In other words, the variability of the inverted barometer effect is seasonal;
- the non-static component of the sea level anomalies has irregular spatial fluctuations and has positive, negative and zero values in different latitudes and most months. Although the range of positive values throughout the region and in most months is more than its negative values which indicates that the barotropic and steric signals tend to form positive sea level anomalies in the Arabian Sea;
- according to the results, the periodic pattern of variation in sea level anomaly with less contribution in total variance that was introduced as the 3rd EOF with 7.2%, can demonstrate the quasi-static sea level changes in the NWIO.

#### REFERENCES

- Antonov J., Levitus S. and Boyer T.; 2005: *Thermosteric sea level rise, 1955-2003*. Geophys. Res. Lett., **32**, 1-4, doi: 10.1029/2005GL023112.
- Barzandeh A., Eshghi N., Hosseinibalam F. and Hassanzadeh S.; 2018: *Wind-driven coastal upwelling along the northern shoreline of the Persian Gulf*. Boll. Geof. Teor. Appl., **59**, 301-312, doi: 10.4430/bgta0235.
- Behera S., Krishnan R. and Yamagata T.; 1999: *Unusual ocean-atmosphere conditions in the tropical Indian Ocean during 1994*. Geophys. Res. Lett., **26**, 3001-3004, doi: 10.1029/1999GL010434.

- Bouttes N., Gregory J., Kuhlbrodt T. and Smith R.; 2014: *The drivers of projected North Atlantic sea level change*. *Clim. Dyn.*, **43**, 1531-1544, doi: 10.1007/s00382-013-1973-8.
- Church J.A., Gregory J.M., Huybrechts P., Kuhn M., Lambeck K., Nhuan M., Qin D. and Woodworth P.; 2001: *Changes in sea level*. In: Houghton J.T., Ding Y., Griggs D.J., Noguer M., Van der Linden P.J., Dai X., Maskell K. and Johnson C.A. (eds): *Climate Change 2001: The Scientific Basis: Contribution of Working Group I to the Third Assessment Report of the Intergovernmental Panel*, pp. 639-694.
- Church J.A., White N.J., Coleman R., Lambeck K. and Mitrovica J.X.; 2004: *Estimates of the regional distribution of sea level rise over the 1950-2000 period*. *J. Clim.*, **17**, 2609-2625, doi: 10.1175/1520-0442(2004)017<2609:EOTRDO>2.0.CO;2.
- Church J.A., White N.J. and Hunter J.R.; 2006: *Sea-level rise at tropical Pacific and Indian Ocean Islands*. *Global Planet. Change*, **53**, 155-168, doi: 10.1016/j.gloplacha.2006.04.001.
- Clemens S., Prell W., Murray D., Shimmield G. and Weedon G.; 1991: *Forcing mechanisms of the Indian Ocean monsoon*. *Nat.*, **353**, 720-725, doi: 10.1038/353720a0.
- Dee D.P., Uppala S., Simmons A., Berrisford P., Poli P., Kobayashi S., Andrae U., Balmaseda M., Balsamo G. and Bauer P.; 2011: *The ERA-Interim reanalysis: configuration and performance of the data assimilation system*. *Quarterly J. R. Meteorol. Soc.*, **137**, 553-597, doi: 10.1002/qj.828.
- Deser C., Alexander M.A., Xie S.-P. and Phillips A.S.; 2010: *Sea surface temperature variability: patterns and mechanisms*. *Ann. Rev. Mar. Sci.*, **2**, 115-143, doi: 10.1146/annurev-marine-120408-151453.
- Dhage L. and Strub P.T.; 2016: *Intra-seasonal sea level variability along the west coast of India*. *J. Geophys. Res. C: Oceans*, **121**, 8172-8188, doi: 10.1002/2016JC011904.
- Douglas B.C.; 1991: *Global sea level rise*. *J. Geophys. Res. C: Oceans*, **96**, 6981-6992, doi: 10.1029/91JC00064.
- Du Y., Xie S.-P., Huang G. and Hu K.; 2009: *Role of air - sea interaction in the long persistence of El Niño - induced north Indian Ocean warming*. *J. Clim.*, **22**, 2023-2038, doi: 10.1175/2008JCLI2590.1.
- Gera A., Mitra A., Mahapatra D., Momin I., Rajagopal E. and Basu S.; 2016: *Sea surface height anomaly and upper ocean temperature over the Indian Ocean during contrasting monsoons*. *Dyn. Atmos. Oceans*, **75**, 1-21, doi: 10.1016/j.dynatmoce.2016.04.002.
- Gill A.E.; 1982: *Atmosphere - ocean dynamics*. Elsevier, New York, NY, USA, 662 pp.
- Goring D.G.; 1995: *Short - term variations in sea level (2-15 days) in the New Zealand region*. *New Zealand J. Mar. Freshwater Res.*, **29**, 69-82, doi: 10.1080/00288330.1995.9516641.
- Gornitz V.; 1995: *Sea - level rise: a review of recent past and near - future trends*. *Earth Surf. Processes Landforms*, **20**, 7-20, doi: 10.1002/esp.3290200103.
- Grachev A., Fairall C., Hare J., Edson J. and Miller S.; 2003: *Wind stress vector over ocean waves*. *J. Phys. Oceanogr.*, **33**, 2408-2429, doi: 10.1175/1520-0485(2003)033<2408:WSVOOW>2.0.CO;2.
- Han W., Meehl G.A., Rajagopalan B., Fasullo J.T., Hu A., Lin J., Large W.G., Wang J.-W., Quan X.-W. and Trenary L.L.; 2010: *Patterns of Indian Ocean sea - level change in a warming climate*. *Nat. Geosci.*, **3**, 546-550, doi: 10.1038/ngeo901.
- Hendon H.H., Liebmann B. and Glick J.D.; 1998: *Oceanic Kelvin waves and the Madden-Julian oscillation*. *J. Atmos. Sci.*, **55**, 88-101, doi: 10.1175/1520-0469(1998)055<0088:OKWATM>2.0.CO;2.
- Jordà G. and Gomis D.; 2013: *On the interpretation of the steric and mass components of sea level variability: the case of the Mediterranean basin*. *J. Geophys. Res. C: Oceans*, **118**, 953-963, doi: 10.1002/jgrc.20060.
- Kumar B.P., Vialard J., Lengaigne M., Murty V. and McPhaden M.J.; 2012: *TropFlux: air - sea fluxes for the global tropical oceans - description and evaluation*. *Clim. Dyn.*, **38**, 1521-1543, doi: 10.1007/s00382-011-1115-0.
- Levitus S., Antonov J.I., Boyer T.P. and Stephens C.; 2000: *Warming of the world ocean*. *Sci.*, **287**, 2225-2229, doi: 10.1126/science.287.5461.2225.
- Li Y. and Han W.; 2015: *Decadal sea level variations in the Indian Ocean investigated with HYCOM: roles of climate modes, ocean internal variability, and stochastic wind forcing*. *J. Clim.*, **28**, 9143-9165, doi: 10.1175/JCLI-D-15-0252.1.
- Mathers E. and Woodworth P.; 2004: *A study of departures from the inverse - barometer response of sea level to air - pressure forcing at a period of 5 days*. *Quarterly J. R. Meteorol. Soc.*, **130**, 725-738, doi: 10.1256/qj.03.46.
- McDougall T.J., Jackett D.R., Wright D.G. and Feistel R.; 2003: *Accurate and computationally efficient algorithms for potential temperature and density of seawater*. *J. Atmos. Oceanic Tech.*, **20**, 730-741, doi: 10.1175/1520-0426(2003)20<730:AACEAF>2.0.CO;2.
- Murtugudde R., McCreary Jr. J.P. and Busalacchi A.J.; 2000: *Oceanic processes associated with anomalous events in the Indian Ocean with relevance to 1997-1998*. *J. Geophys. Res. C: Oceans*, **105**, 3295-3306, doi: 10.1029/1999JC900294.

- Parekh A., Gnanaseelan C., Deepa J., Karmakar A. and Chowdary J.; 2017: *Sea level variability and trends in the north Indian Ocean*. In: Rajeevan M.N. and Nayak S. (eds), *Observed Climate Variability and Change over the Indian Region*, Springer, Singapore, pp. 181-192.
- Piecuch C.G. and Ponte R.M.; 2015: *Inverted barometer contributions to recent sea level changes along the northeast coast of North America*. *Geophys. Res. Lett.*, **42**, 5918-5925, doi: 10.1002/2015GL064580.
- Piecuch C.G., Dangendorf S., Ponte R.M. and Marcos M.; 2016a: *Annual sea level changes on the North American northeast coast: influence of local winds and barotropic motions*. *J. Clim.*, **29**, 4801-4816, doi: 10.1175/JCLI-D-16-0048.1.
- Piecuch C.G., Thompson P.R. and Donohue K.A.; 2016b: *Air pressure effects on sea level changes during the twentieth century*. *J. Geophys. Res. C: Oceans*, **121**, 7917-7930, doi: 10.1002/2016JC012131.
- Ponte R.M.; 2006: *Low-frequency sea level variability and the inverted barometer effect*. *J. Atmos. Oceanic Tech.*, **23**, 619-629, doi: 10.1175/JTECH1864.1.
- Qasim S.; 1982: *Oceanography of the northern Arabian Sea*. *Deep Sea Res. Part A*, **29**, 1041-1068, doi: 10.1016/0198-0149(82)90027-9.
- Roberts C., Calvert D., Dunstone N., Hermanson L., Palmer M. and Smith D.; 2016: *On the drivers and predictability of seasonal - to - interannual variations in regional sea level*. *J. Clim.*, **29**, 7565-7585, doi: 10.1175/JCLI-D-15-0886.1.
- Roquet F., Madec G., McDougall T.J. and Barker P.M.; 2015: *Accurate polynomial expressions for the density and specific volume of seawater using the TEOS-10 standard*. *Ocean Modell.*, **90**, 29-43, doi: 10.1016/j.ocemod.2015.04.002.
- Ruiz Echeverry L., Saraceno M., Piola A. and Strub P.; 2016: *Sea level anomaly on the Patagonian continental shelf: trends, annual patterns and geostrophic flows*. *J. Geophys. Res. C: Oceans*, **121**, 2733-2754, doi: 10.1002/2015JC011265.
- Saji N., Goswami B., Vinayachandran P. and Yamagata T.; 1999: *A dipole mode in the tropical Indian Ocean*. *Nat.*, **401**, 360-363, doi: 10.1038/43854.
- Schott F.A., Xie S.P. and McCreary J.P.; 2009: *Indian Ocean circulation and climate variability*. *Rev. Geophys.*, **47**, RG1002, doi: 10.1029/2007RG000245.
- Sengupta D., Senan R. and Goswami B.; 2001: *Origin of intraseasonal variability of circulation in the tropical central Indian Ocean*. *Geophys. Res. Lett.*, **28**, 1267-1270, doi: 10.1029/2000GL012251.
- Shankar D. and Shetye S.; 1999: *Are interdecadal sea level changes along the Indian coast influenced by variability of monsoon rainfall?* *J. Geophys. Res. C: Oceans*, **104**, 26031-26042, doi: 10.1029/1999JC900218.
- Shetye S., Gouveia A., Shenoi S., Michael G., Sundar D., Almeida A. and Santanam K.; 1991: *The coastal current off western India during the northeast monsoon*. *Deep Sea Res. Part A*, **38**, 1517-1529 doi: 10.1016/0198-0149(91)90087-V.
- Shetye S., Gouveia A. and Shenoi S.; 1994: *Circulation and water masses of the Arabian Sea*. *J. Earth Syst. Sci.*, **103**, 107-123 doi: 10.1007/BF02839532.
- Shukla J.; 1987a: *Interannual variability of monsoons*. In: Fein J.S. and Stephens P.L. (eds), *Monsoons*, John Wiley and Sons, New York, NY, USA, pp. 399-464.
- Shukla J.; 1987b: *Long-range forecasting of monsoons*. In: Fein J.S. and Stephens P.L. (eds), *Monsoons*, John Wiley and Sons, New York, NY, USA, pp. 523-548.
- Soumya M., Vethamony P. and Tkalich P.; 2015: *Inter - annual sea level variability in the southern South China Sea*. *Global Planet. Change*, **133**, 17-26, doi: 10.1016/j.gloplacha.2015.07.003.
- Stammer D., Cazenave A., Ponte R.M. and Tamisiea M.E.; 2013: *Causes for contemporary regional sea level changes*. *Annu. Rev. Mar. Sci.*, **5**, 21-46, doi: 10.1146/annurev-marine-121211-172406.
- Sturges W. and Douglas B.C.; 2011: *Wind effects on estimates of sea level rise*. *J. Geophys. Res. C: Oceans*, **116**, C06008, doi: 10.1029/2010JC006492.
- Timmermann A., McGregor S. and Jin F.F.; 2010: *Wind effects on past and future regional sea level trends in the southern Indo-Pacific*. *J. Clim.*, **23**, 4429-4437, doi: 10.1175/2010JCLI3519.1.
- Unnikrishnan A. and Shankar D.; 2007: *Are sea - level - rise trends along the coasts of the north Indian Ocean consistent with global estimates?* *Global Planet. Change*, **57**, 301-307, doi: 10.1016/j.gloplacha.2006.11.029.
- Unnikrishnan A., Kumar K.R., Fernandes S.E., Michael G. and Patwardhan S.; 2006: *Sea level changes along the Indian coast: observations and projections*. *Curr. Sci.*, **90**, 362-368, < drs.nio.org/drs/handle/2264/156 >.
- Venzke S., Latif M. and Villwock A.; 2000: *The coupled GCM ECHO-2. Part II: Indian ocean response to ENSO*. *J. Clim.*, **13**, 1371-1383, doi: 10.1175/1520-0442(2000)013<1371:TCGE>2.0.CO;2.
- Webster P.J., Magana V.O., Palmer T., Shukla J., Tomas R., Yanai M. and Yasunari T.; 1998: *Monsoons: processes, predictability, and the prospects for prediction*. *J. Geophys. Res. C: Oceans*, **103**, 14451-14510, doi: 10.1029/97JC02719.

- Wu Q., Zhang X., Church J.A. and Hu J.; 2017: *Variability and change of sea level and its components in the Indo - Pacific region during the altimetry era*. J. Geophys. Res. C: Oceans, **122**, 1862-1881, doi: 10.1002/2016JC012345.
- Wunsch C. and Stammer D.; 1997: *Atmospheric loading and the oceanic "inverted barometer" effect*. Rev. Geophys., **35**, 79-107, doi: 10.1029/96RG03037.
- Yamagata T., Behera S.K., Luo J.J., Masson S., Jury M.R. and Rao S.A.; 2004: *Coupled ocean - atmosphere variability in the tropical Indian Ocean*. Earth's Climate: The Ocean - Atmosphere Interaction, Geophys. Monogr. Ser., **147**, 189-212. doi: 10.1029/147GM12.

*Corresponding author:* Fahimeh Hosseinibalam  
Department of Physics, University of Isfahan  
Isfahan 81746-73441, Iran  
Phone: + 98 313 7934733; e-mail: fhb@sci.ui.ac.ir